Supporting Information

Cerium oxide nanozyme attenuates periodontal bone destruction by inhibiting ROS-NFκB pathway

Yijun Yu[#a], Sheng Zhao[#b], Deao Gu[c], Bijun Zhu[a], Hanxiao Liu[a], Wenlei Wu[d], Jiangjiexing Wu[*b, e], Hui Wei[*b], Leiying Miao[*a]

[a] Department of Cariology and Endodontics, Nanjing Stomatological Hospital, Medical School of Nanjing University, Nanjing, Jiangsu 210008, China.

[b] Department of Biomedical Engineering, College of Engineering and Applied Sciences, Nanjing National Laboratory of Microstructures, Jiangsu Key Laboratory of Artificial Functional Materials, Chemistry and Biomedicine Innovation Center (ChemBIC), Nanjing University, Nanjing, Jiangsu 210023, China.

[c] Department of Orthodontics, Nanjing Stomatological Hospital, Medical School of Nanjing University, Nanjing, Jiangsu 210008, China.

[d] Nanjing Stomatological Hospital, Medical School of Nanjing University, Nanjing, Jiangsu 210008, China.

[e] School of Marine Science and Technology, Tianjin University, Tianjin 300072, China.

Corresponding Authors

[*] E-mail:

miaoleiying80@163.com

weihui@nju.edu.cn

wujiangjiexing2007@126.com

[#] These authors contributed to this work equally.

Materials

Cerium nitrate hexahydrate, ethylene glycol, and ammonia solution were obtained from Aladdin. 2',7'-dichlorofluorodiacetate (DCFH-DA) probe and lipopolysaccharide (LPS) were purchased from Sigma. Dulbecco's modified Eagle medium (DMEM), fetal bovine serum (FBS), penicillin and streptomycin solution were purchased from Gibco. CCK-8 solution was purchased from Dojindo. HEPES buffered Krebs-Ringer solution was purchased from Tiandz, Inc. The assay kits and antibodies used were listed in Table S2.

Instrumentations

Transmission electron microscope (TEM) images were detected on a JEM-2100 TEM (JEOL, Japan). The X-ray diffraction (XRD) patterns were obtained on a diffractometer (X'TRA, Thermo Fisher Scientific, USA) using a Cu Kα radiation. X-ray photoelectron spectroscopy (XPS) was examined using a PHI 5000 VersaProbe (ULVAC-PHI, Japan). All the absorbance data were collected on a Spectra Max M3 microplate reader (Molecular Device, USA). Fluorescence images were obtained by a confocal microscopy (Nikon Ti, Japan). All the maxillary specimens were scanned with a micro-CT system (Skyscan 1176; Skyscan, Belgium).

Synthesis and characterization of CeO_2 nanoparticles

The synthesis of CeO_2 NPs was performed as described previously.[1, 2] Briefly, cerium nitrate hexahydrate (5.8 mmol) was dissolved in a 1:1 mixture of water and ethylene glycol. The solution was heated to 60 ℃ under magnetic stirring and 16 mL of aqueous ammonia (25%) was added to the mixture for 3 h. Then, the CeO_2 NPs were obtained by centrifugation (10000 r/min). In order to remove the residual reagents, the products were washed with deionized water, and treated with citric acid by ultrasound. Subsequently, the pH of citrate modified CeO_2 NP solution was adjusted to about 7.0. At last, the CeO_2 solutions were centrifugated, and re-dissolved in water or freeze-dried for further applications,

The morphology of CeO_2 NPs was evaluated via TEM imaging. The solution was dropped onto a copper net with a supportive carbon film adhesion and then left to dry before observation. Dynamic light scattering (DLS) was used to measure hydrated CeO_2 nanoparticle size. XRD was performed to determine the phase composition and crystallinity of synthetic powders. Powders were scanned from 20 – 80 ° using Cu-Ka radiation at a scanning speed of 5° per min. XPS was used to discern

the valence state distribution of Ce.

Cytotoxicity analysis of CeO_2 NPs

RAW 264.7 cells were purchased from the National Collection of Authenticated Cell Cultures and cultured in a medium composed of high-glucose DMEM (supplemented with 5% FBS, 1% penicillin and streptomycin) in an incubator at 5% CO_2 and 37 ℃. Cells were seeded into 96-well plates at a density of 5×10^3 per well. After cellular adhesion to the wells, different concentrations of CeO_2 NPs (0 – 1000 μg/mL) were added to the wells. After incubation for 24 h, CCK-8 solution (10 μL) and DMEM (90 μL) were added to the plate. Absorbance was then measured at 450 nm using a UV/VIS spectrophotometer after incubation for a further 2 h at 37℃.

Detection of intracellular ROS level induced by LPS

RAW 264.7 cells were seeded into glass-bottom dishes at a density of 5×10^4 per dish for observation under a confocal microscopy. Cells were treated with 20 and 100 ng/mL of LPS solution for 12 and 18 h, then washed twice with PBS and incubated with a 10 μM DCFH-DA probe for 5 – 10 min. Importantly, cells were washed with HEPES Buffered Krebs-Ringer solution after probe loading and before observation.

In vitro anti-inflammatory and anti-oxidative studies

Total RNA extraction was performed in accordance with conventional methods and 1 μg of total RNA was used for reverse transcription to obtain cDNA with a kit from Vazyme Biotech (HiScript III RT SuperMix for qPCR (+gDNA wiper)). Real-time quantitative PCR was performed on a StepOne™ real-time PCR system using ChamQ Universal SYBR qPCR Master Mix (Vazyme Biotech). Data were analyzed using the $2^{-\Delta\Delta CT}$ method and normalized to GAPDH. Primer sequences are listed in Table S1.

Total cellular proteins were extracted using RIPA buffer supplemented with a protease inhibitor cocktail (Beyotime Biotechnology). Protein samples were loaded and separated by SDS-PAGE electrophoresis, then transferred onto PVDF membranes (Millipore). After blocking with 5% skim milk for 1 h at room temperature, membranes with different target proteins were incubated with primary antibodies such as iNOS (Cell Signalling Technology, 1:1000), HO-1 (Proteintech, 1:1000) and Nrf2 (Abcam, 1:500) overnight at 4 ℃. β-Tubulin (Bioworld, 1:5000) was used as an internal reference. Before incubation with secondary antibodies for 1 h at room temperature, membranes were washed with TBST three times to eliminate nonspecific binding. Finally, the membranes were

immersed in a chemiluminescent reagent (Vazyme Biotech) and target protein bands were visualized using a Tanon imaging system.

***In vivo* ROS scavenging activity of CeO_2 NPs**

Sprague Dawley rats weighing about 240 g were chosen for the establishment of a model of gingival inflammation. LPS (1 mg/mL; 25 μL) was injected into the buccal gingiva of the lower front teeth daily. After 3 d of administration, CeO_2 NPs (2 mg/mL; 25 μL) were injected. Then, DCFH-DA was injected to quantify levels of ROS induced by LPS after 24 h. Fluorescence imaging was performed using a small animal imaging system (n = 3). Untreated rats were defined as controls.

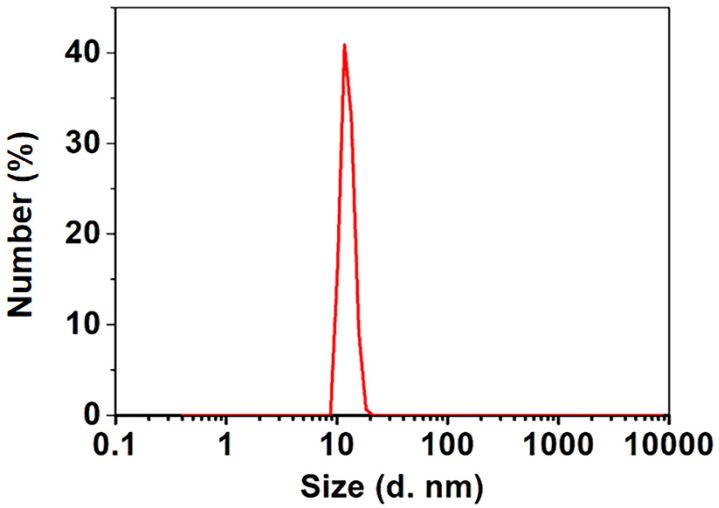

Fig. S1 The DLS analysis of CeO_2 NPs.

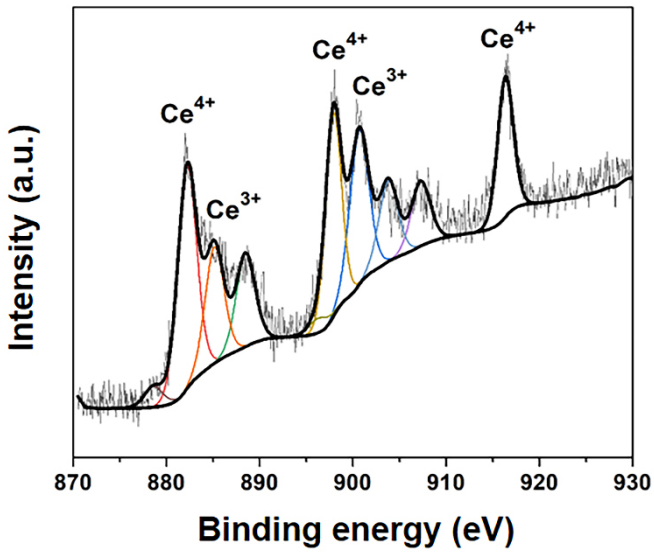

Fig. S2 XPS spectrum of CeO_2 NPs.

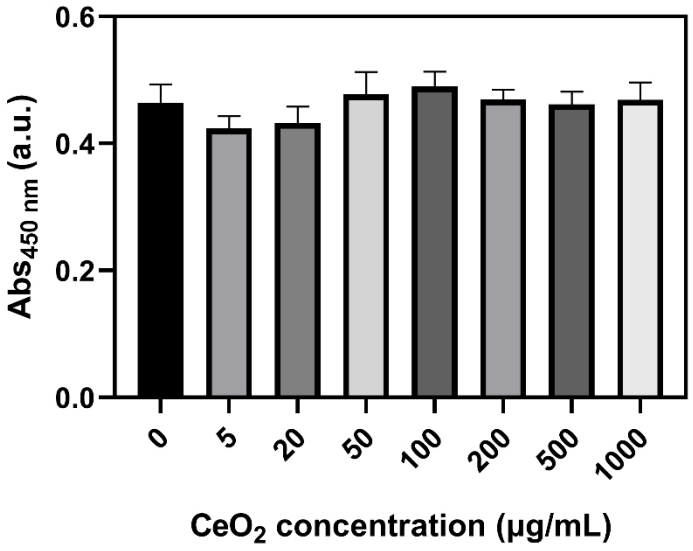

Fig. S3 The biocompatibility of CeO_2 NPs. There showed no obvious significant effect on survival vitality of RAW 264.7 cells.

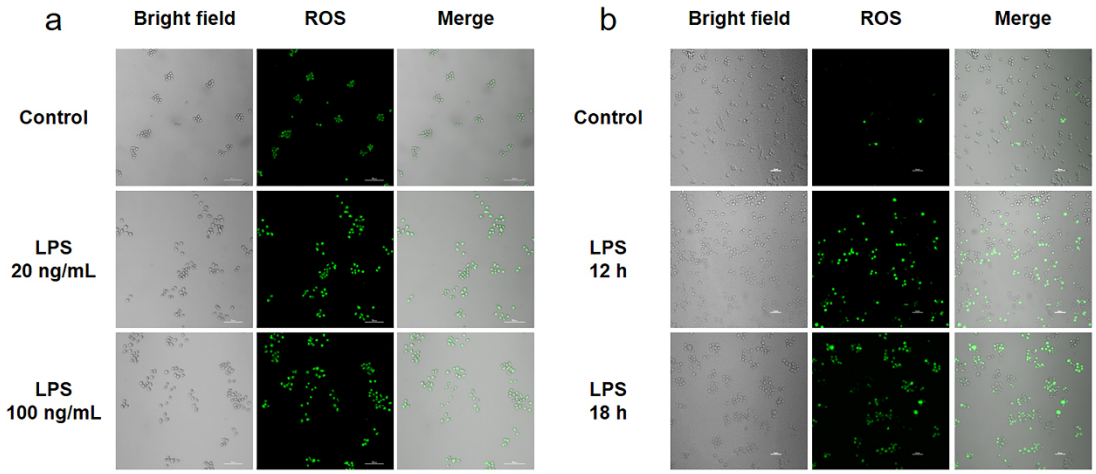

Fig. S4 The intracellular ROS level with different treatments. a. Induced by different concentrations of LPS for 12 h, b. induced by LPS at 20 ng/mL for different times. Scale bar: 50 μm.

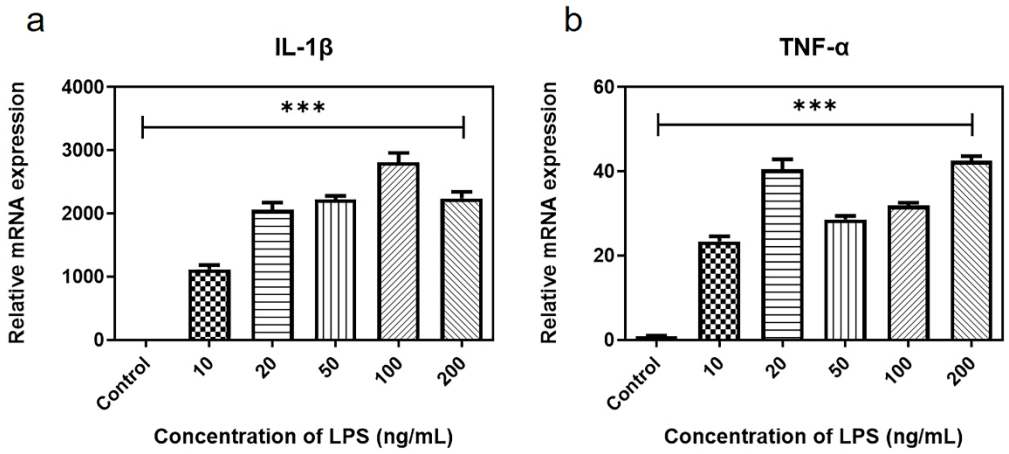

Fig. S5 The relative mRNA expression of IL-1β and TNF-α in RAW 264.7 with different concentrations of LPS for 3 h. *** means $P < 0.001$.

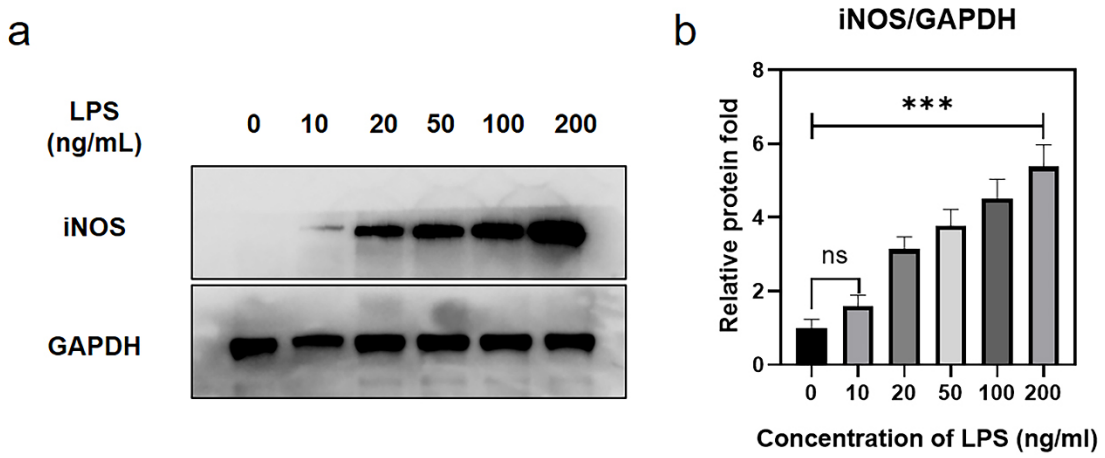

Fig. S6 The iNOS protein expression in RAW 264.7 with different concentrations of LPS for 18 h. a, Western blot bands; b, normalized protein level of iNOS. *** means $P < 0.001$.

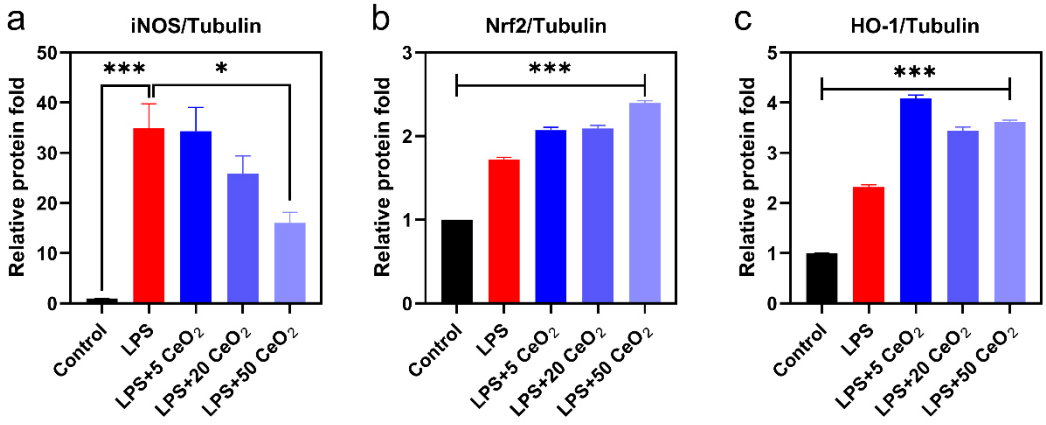

Fig. S7 The normalized values of the Western blot bands in Fig. 3d. *** means $P < 0.001$, * means $P < 0.05$.

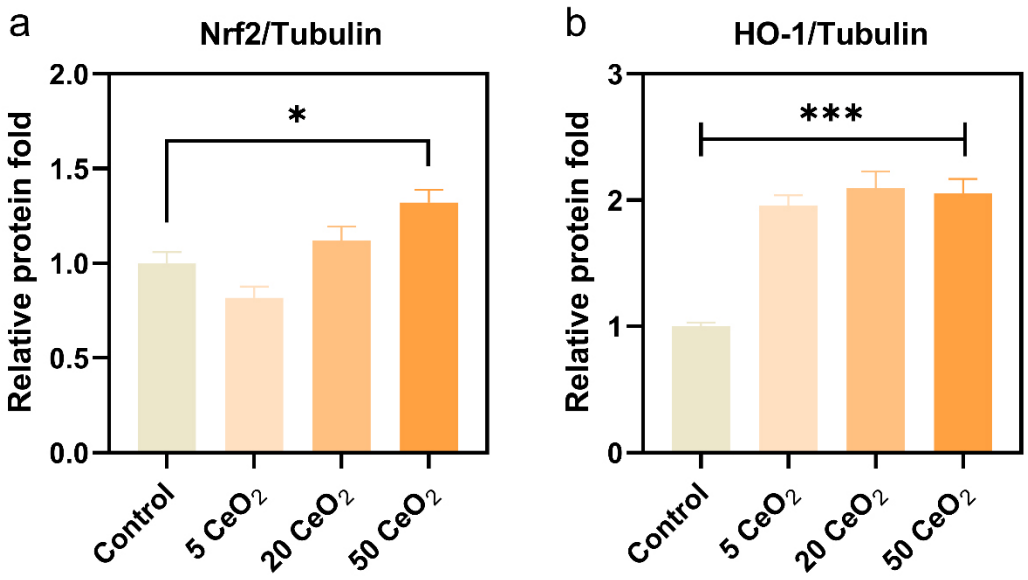

Fig. S8 The normalized values of the Western blot bands in Fig. 3 e.*** means $P < 0.001$, * means $P < 0.05$.

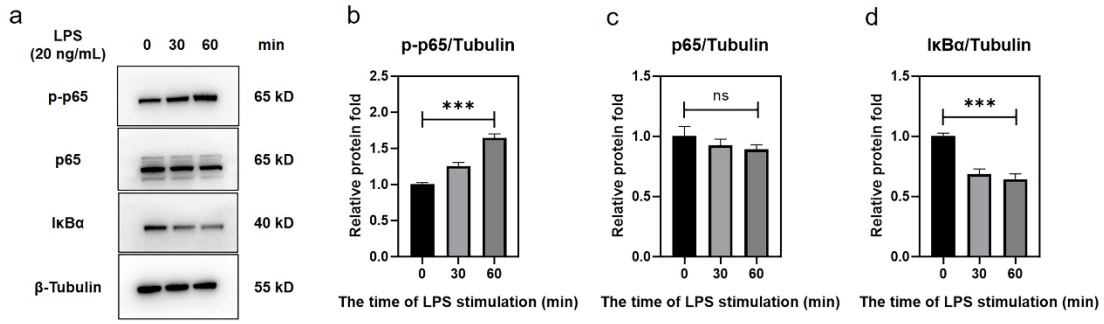

Fig. S9 The expression of NFκB related key proteins activated by LPS at different time. a, Western blot bands; b, normalized protein level of p-p65; c, normalized protein level of p65; d, normalized protein level of IκBα. *** means $P < 0.001$.

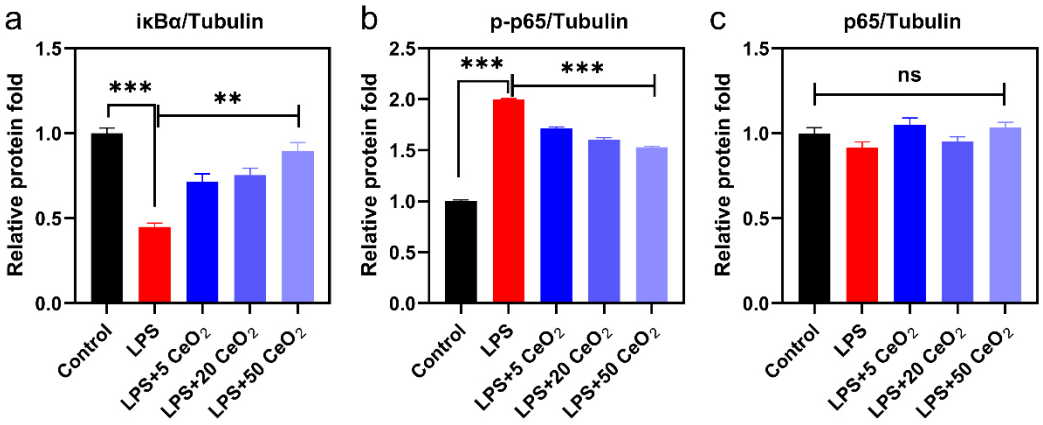

Fig. S10 The normalized values of the Western blot bands in Fig. 4a. *** means $P < 0.001$, ** means $P < 0.01$, ns means $P > 0.05$.

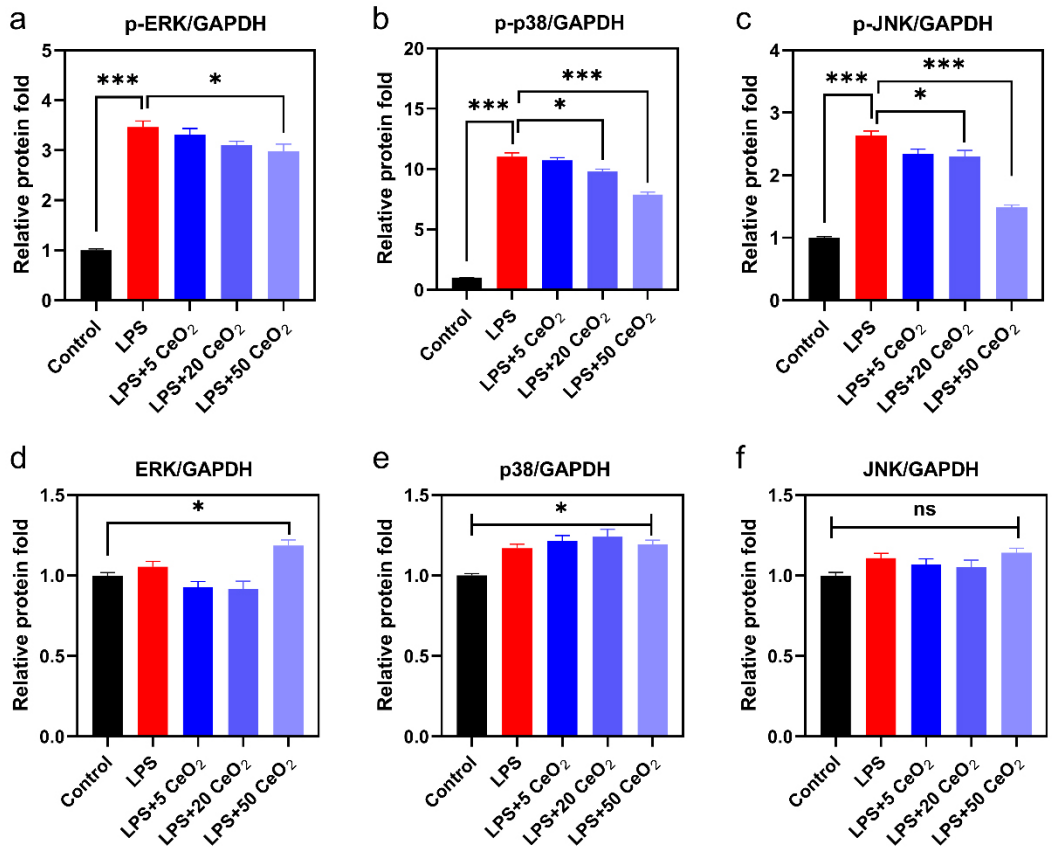

Fig. S11 The normalized values of the Western blot bands in Fig. 4 b. *** means $P < 0.001$, * means $P < 0.05$, ns means $P > 0.05$.

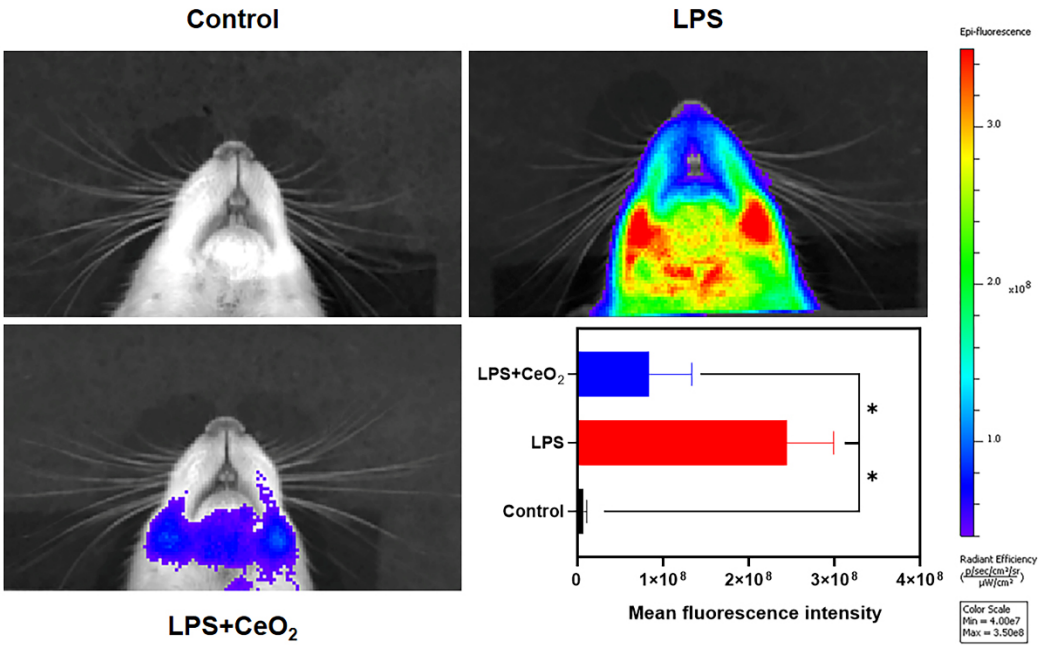

Fig. S12 *In vivo* fluorescence imaging of rat with LPS-induced gingival inflammation. * means $P <$ 0.05.

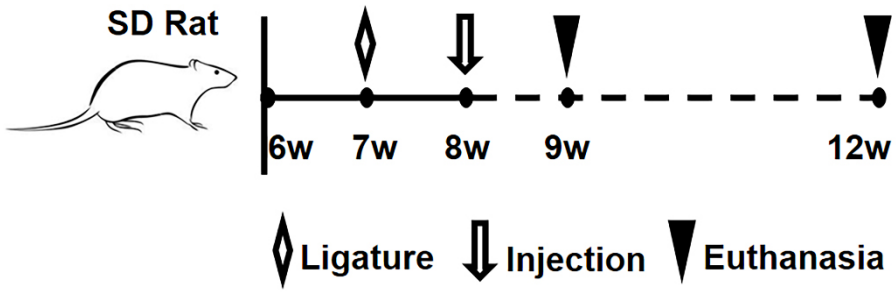

Fig. S13 The time chart in establishing the rat periodontitis model.

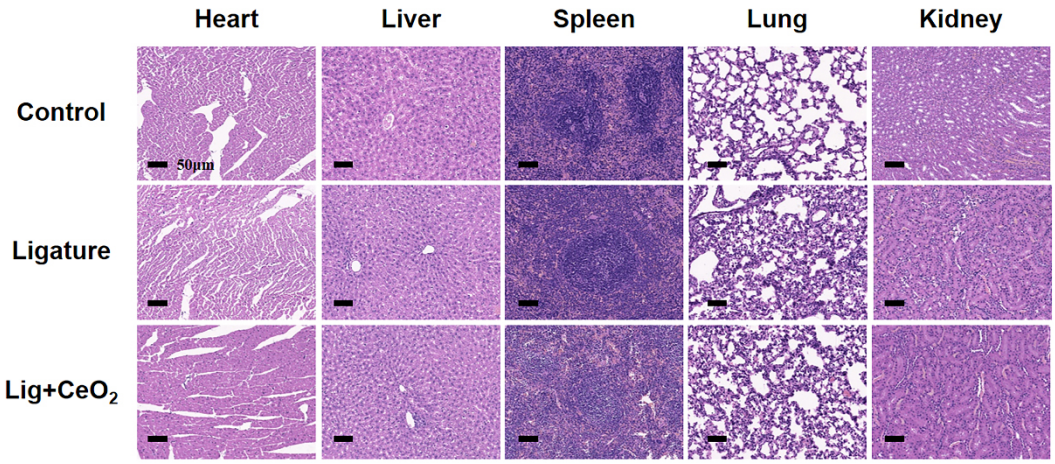

Fig. S14 The histological sections of vital viscera. Scale bar: 50 μm.

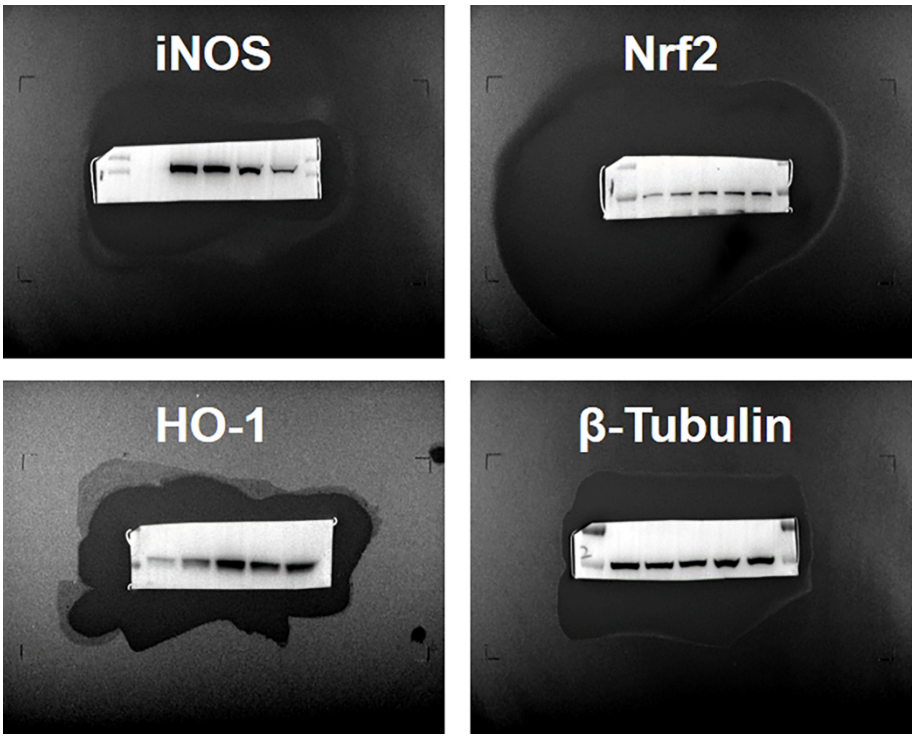

Fig. S15 Original WB scans for Fig. 3 d.

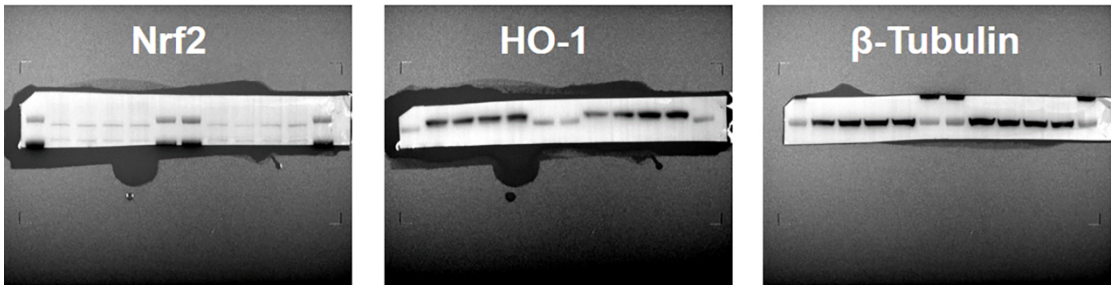

Fig. S16 Original WB scans for Fig. 3 e.

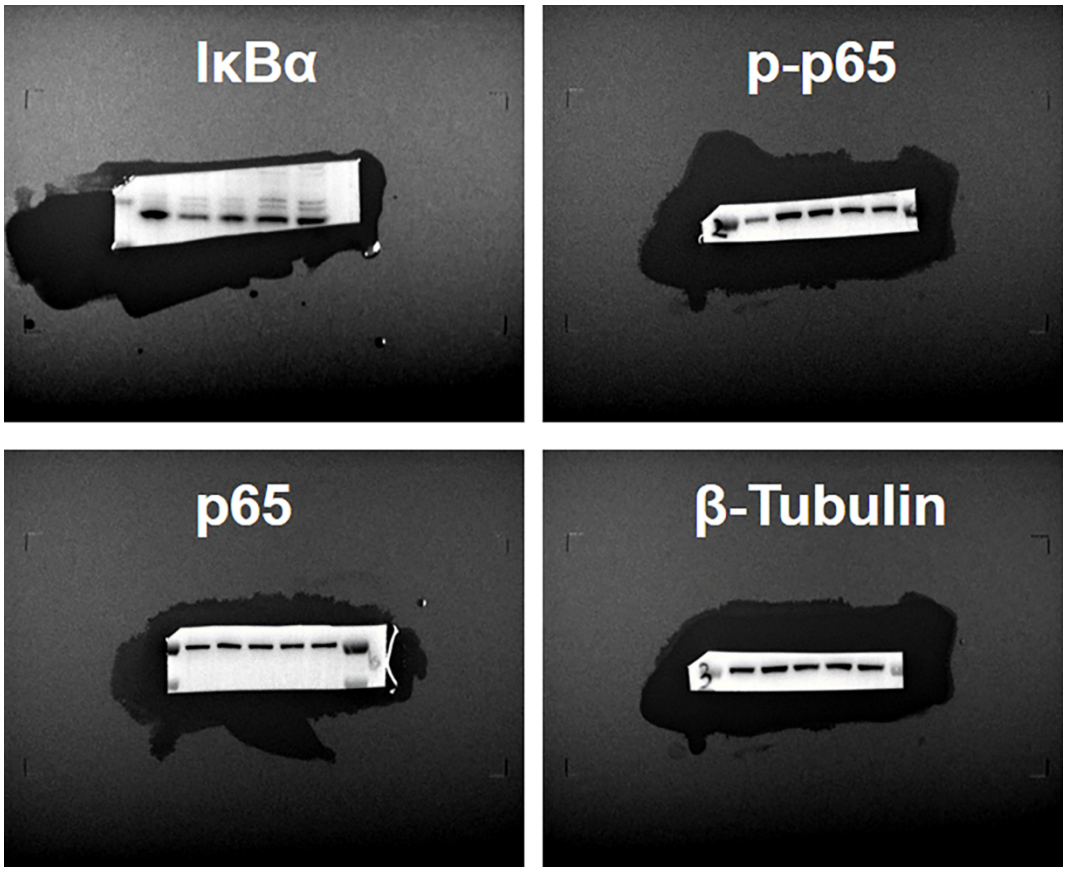

Fig. S17 Original WB scans for Fig. 4 a.

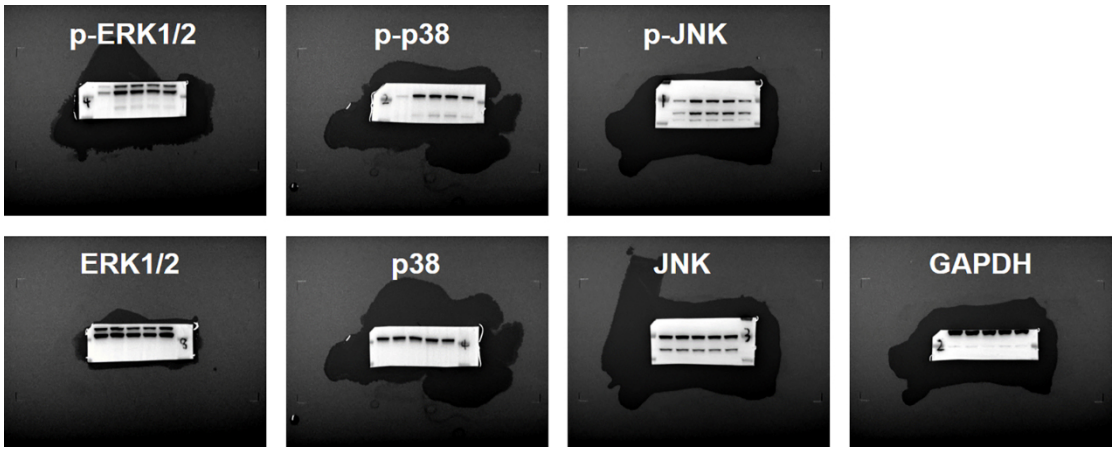

Fig. S18 Original WB scans for Fig. 4 b.

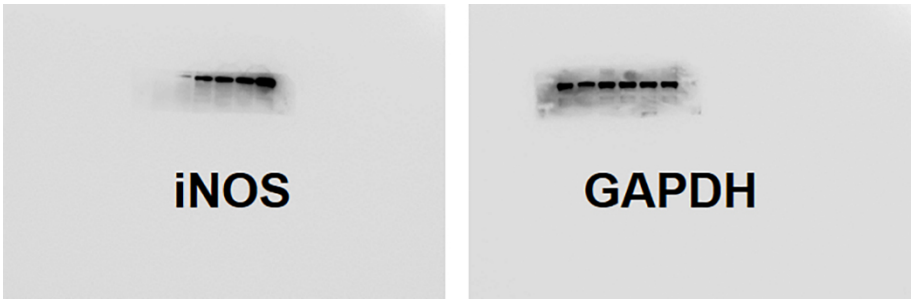

Fig. S19 Original WB scans for Fig. S6.

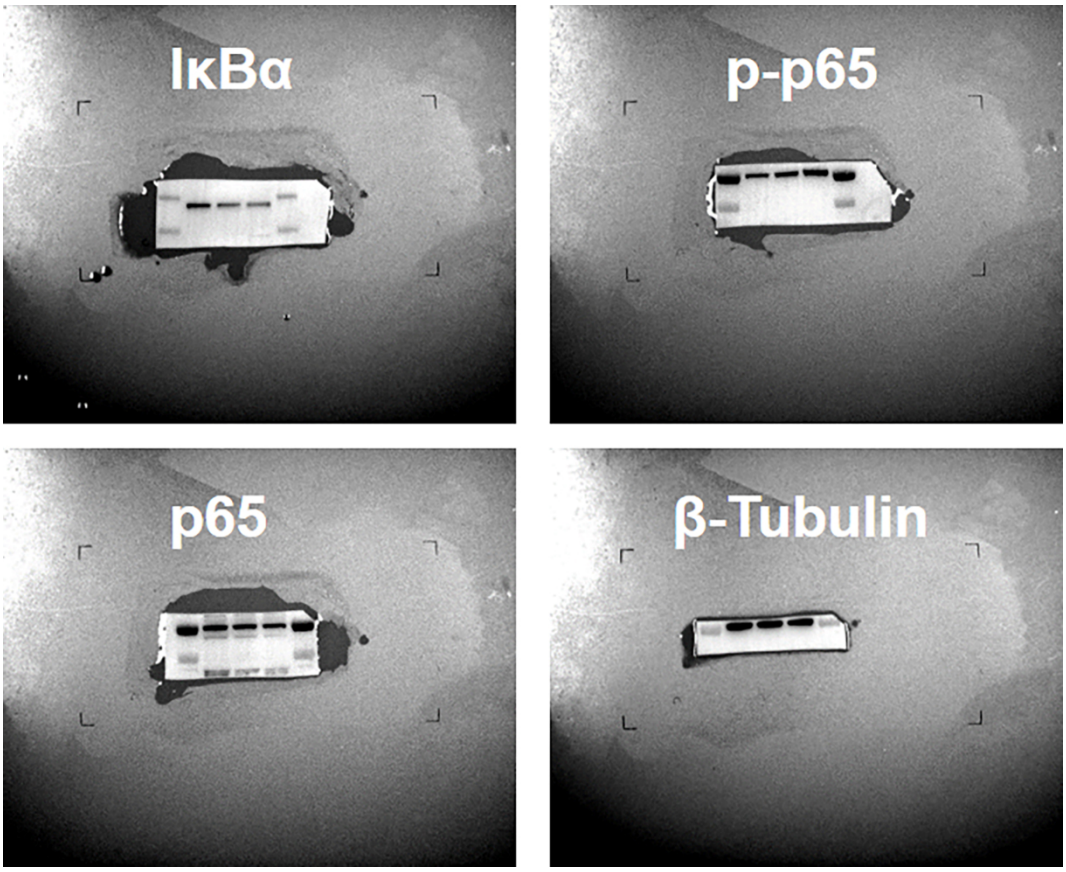

Fig. S20 Original WB scans for Fig. S9.

Table S1 The sequences of primers

Gene （mouse）	**Primer sequence**	
HO-1	Forward	AGGTACACATCCAAGCCGAGA
	Reverse	CATCACCAGCTTAAAGCCTTCT
NQO1	Forward	AGGATGGGAGGTACTCGAATC
	Reverse	TGCTAGAGATGACTCGGAAGG
Gclc	Forward	CTACCACGCAGTCAAGGACC
	Reverse	CCTCCATTCAGTAACAACTGGAC
Gclm	Forward	AGGAGCTTCGGGACTGTATCC
	Reverse	GGAAACTCCCTGACTAAATCGG
IL-1β	Forward	GAAATGCCACCTTTTGACAGTG
	Reverse	TGGATGCTCTCATCAGGACAG
TNF-α	Forward	CAGGCGGTGCCTATGTCTC
	Reverse	CGATCACCCCGAAGTTCAGTAG
iNOS	Forward	GTTCTCAGCCCAACAATACAAGA
	Reverse	GTGGACGGGTCGATGTCAC
GAPDH	Forward	AGGTCGGTGTGAACGGATTTG
	Reverse	GGGGTCGTTGATGGCAACA

Table S2 The assay kits and antibodies used in this study

Product name	**Company**	**Country**
SOD Assay kit-WST	Dojindo	Japan
Hydroxyl radical assay kit	Jiancheng Bioengineering Institute	China
HiScript III RT SuperMix for qPCR (+gDNA wiper)	Vazyme Biotech	China
iNOS, p38, p-p38, ERK1/2, p-ERK1/2, JNK, and p-JNK antibodies	Cell Signalling Technology	USA
Nrf2 antibody	Abcam	USA
HO-1 antibody	Proteintech	USA
β-Tubulin, GAPDH antibody	Bioworld	China
p-p65, p65, and IκBα antibodies	Affinity Biosciences	USA
Alexa Fluor 488-conjugated secondary antibody	ThermoFisher Scientific	USA

References

1. H. Cheng, S. Lin, F. Muhammad, Y.-W. Lin and H. Wei, *ACS Sens.*, 2016, **1**, 1336-1343.
2. S. Zhao, Y. X. Li, Q. Y. Liu, S. R. Li, Y. Cheng, C. Q. Cheng, Z. Y. Sun, Y. Du, C. J. Butch and H. Wei, *Adv. Funct. Mater.*, 2020, **30**, 2004692.